On the Metallic Conductivity of the Delafossites $PdCoO_2$ and $PtCoO_2$

Volker Eyert,* Raymond Frésard, and Antoine Maignan

Laboratoire CRISMAT, UMR CNRS-ENSICAEN(ISMRA) 6508, 6 Boulevard Maréchal Juin, 14050 Caen Cedex, France

Received December 4, 2007. Revised Manuscript Received January 18, 2008

The origin of the quasi two-dimensional behavior of $PdCoO_2$ and $PtCoO_2$ is investigated by means of electronic structure calculations. They are performed using density functional theory in the generalized gradient approximation as well as the new full-potential augmented spherical wave method. We show that the electric conductivity is carried almost exclusively by the in-plane Pd (Pt) d orbitals. In contrast, the insulating CoO_2 sandwich layers of octahedrally coordinated Co atoms may be regarded as charge carrier reservoirs. This leads to a weak electronic coupling of the Pd (Pt) layers. The obtained nearly cylindrical Fermi surface causes the strong anisotropy of the electric conductivity.

1. Introduction

Transition-metal oxides attract a lot of attention due to a great variety of physical phenomena, most of which go along with the ordering of some microscopic degrees of freedom as a function of, for example, temperature, pressure, or doping. Prominent examples are the striking metal–insulator transitions of the vanadates,[1] high-T_c superconductivity in the cuprates, or the colossal magnetoresistance observed in the manganates.[2–5] Cobaltates have aroused much interest due to the occurrence of different spin states.[6–8] In addition, they are promising materials for thermoelectric applications.[9,10]

Known since 1873, when Friedel discovered the mineral $CuFeO_2$, the delafossites ABO_2 keep on generating a strong and ever increasing interest,[11–13] especially after Kawazoe et al. evidenced simultaneous transparency and p-type conductivity,[14] which laid ground for the development of transparent optoelectronic devices. Furthermore, the quasi two-dimensionality of the lattice and the triangular coordination of atoms gave rise to such exciting physical properties as strong anisotropies of the electrical conductivity and magnetic frustration effects.

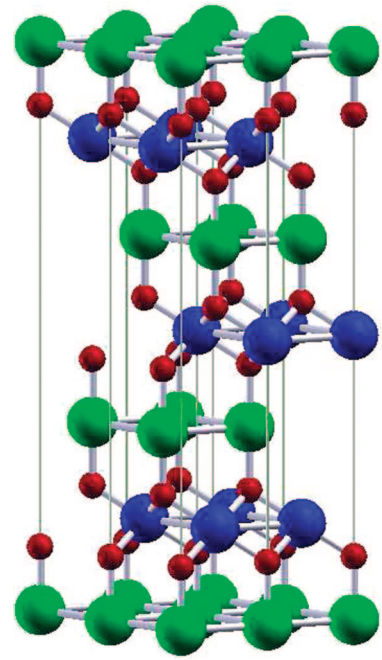

Figure 1. Crystal structure of $PdCoO_2$. Palladium, cobalt, and oxygen atoms are shown as green, blue, and red spheres, respectively.

The delafossite structure has the space group $R\bar{3}m$ and results from a stacking of monatomic triangular layers, see Figure 1.[11,13] In particular, the B-atoms are at the centers of distorted oxygen octahedra, which share edges and form the characteristic BO_2 sandwich layers. These trilayers are

* Corresponding author. E-mail: eyert@physik.uni-augsburg.de. Permanent address: Center for Electronic Correlations and Magnetism, Institut für Physik, Universität Augsburg, 86135 Augsburg, Germany.

(1) Imada, M.; Fujimori, A.; Tokura, Y. *Rev. Mod. Phys.* **1998**, *70*, 1039.
(2) von Helmolt, R.; Wecker, J.; Holzapfel, B.; Schultz, L.; Samwer, K. *Phys. Rev. Lett.* **1993**, *71*, 2331.
(3) Tomioka, Y.; Asamitsu, A.; Moritomo, Y.; Kuwahara, H.; Tokura, Y. *Phys. Rev. Lett.* **1995**, *74*, 5108.
(4) Raveau, B.; Maignan, A.; Caignaert, V. *J. Solid State Chem.* **1995**, *117*, 424.
(5) Maignan, A.; Simon, C.; Caignaert, V.; Raveau, B. *Solid State Commun.* **1995**, *96*, 623.
(6) Eyert, V.; Laschinger, C.; Kopp, T.; Frésard, R. *Chem. Phys. Lett.* **2004**, *385*, 249.
(7) Frésard, R.; Laschinger, C.; Kopp, T.; Eyert, V. *Phys. Rev. B* **2004**, *69*, 140405(R).
(8) Wu, H.; Haverkort, M. W.; Hu, Z.; Khomskii, D. I.; Tjeng, L. H. *Phys. Rev. Lett.* **2005**, *95*, 186401.
(9) Terasaki, I.; Sasago, Y.; Uchinokura, K. *Phys. Rev. B* **1997**, *56*, R12685.
(10) Masset, A. C.; Michel, C.; Maignan, A.; Hervieu, M.; Toulemonde, O.; Studer, F.; Raveau, B. *Phys. Rev. B* **2000**, *62*, 166.
(11) (a) Shannon, R. D.; Rogers, D. B.; Prewitt, C. T. *Inorg. Chem.* **1971**, *10*, 713. (b) Prewitt, C. T.; Shannon, R. D.; Rogers, D. B. *Inorg. Chem.* **1971**, *10*, 719. (c) Rogers, D. B.; Shannon, R. D.; Prewitt, C. T.; Gillson, J. L. *Inorg. Chem.* **1971**, *10*, 723.
(12) Tanaka, M.; Hasegawa, M.; Higuchi, T.; Tsukamoto, T.; Tezuka, Y.; Shin, S.; Takei, H. *Physica B* **1998**, *245*, 157.
(13) Marquardt, M. A.; Ashmore, N. A.; Cann, D. P. *Thin Solid Films* **2006**, *496*, 146.
(14) Kawazoe, H.; Yasukawa, M.; Hyodo, H.; Kurita, M.; Yanagi, H.; Hosono, H. *Nature* **1997**, *389*, 939.

10.1021/cm703404e CCC: $40.75
Published on Web 02/28/2008

interlinked by linear O−A−O bonds, resulting in a 2-fold coordination of the A-atoms. However, the latter have, in addition, six in-plane nearest neighbor A-atoms. For this reason, the structure may be likewise regarded as formed from single A-atom layers, which are intertwined by the octahedral sandwiches. For $PdCoO_2$ and $PtCoO_2$, we will find this latter point of view particularly useful. Finally, the oxygen atoms are tetrahedrally coordinated by one A-atom and three B-atoms. Pressure studies reveal an increase of the structural anisotropy on compression indicating the high mechanical stability of both the octahedral sandwich layers and the O−Pd−O (O−Pt−O) dumbbells.[15]

In general, interest in the delafossite-type compounds has concentrated quite much on the triangular arrangement of the transition-metal atoms and the resulting possible frustration effects, which arise once localized magnetic moments are established. Although most of these oxides have been found to be antiferromagnetic semiconductors, other class members like $PdCrO_2$, $PdCoO_2$, $PdRhO_2$, and $PtCoO_2$ attracted interest because of their rather high metallic conductivity. In particular, $PdCoO_2$ has been shown to possess one of the lowest electric resistivities of normal-state oxides, even lower than that of Pd metal at room temperature.[11,12,16] Yet, the conductivity is strongly anisotropic.[11,16] In particular, the ratio of the resistivities parallel and perpendicular to the *c* axis can be as large as 200 in $PdCoO_2$.[16] Photoemission data indicate that the density of states at the Fermi energy can be exclusively attributed to the Pd 4d states.[12,17,13] From the combination of photoemission spectroscopy and inverse photoemission spectroscopy, several authors concluded that the Fermi energy is located at a shallow minimum of the density of states and doping might thus lead to rather high values of the thermoelectric power.[17,16,18]

Despite their simple chemical formulas the delafossites may be regarded as prototypical superlattices where the composition of both the A and B layers can be used to strongly influence the behavior of the whole system. For instance, in $CuCrO_2$, the Fermi energy falls into the Cr 3d band, but because the Cr layers order magnetically, this compound is a magnetic semiconductor. In contrast, as will be shown below, in $PdCoO_2$, the Co layers only act a charge reservoirs, and conduction takes place almost exclusively in the Pd layers.

As a matter of fact, quite a few electronic structure calculations for delafossites and related compounds have been reported in the literature.[19–23,25,24,26–28] For $PdCoO_2$, there exist linear muffin-tin orbitals calculations by Seshadri et al. as well as by Okabe et al.[21,25] Although according to the former authors, who also investigated $PtCoO_2$, the density of states at E_F is mainly due to the Pd 4d states with only small contributions from the Co 3d and O 2p orbitals, the results by Okabe et al. are not very specific in this respect. For this reason, the role of these orbitals for the metallic conductivity is not yet completely clear. To resolve the issue and to make a closer connection with the photoemission data, we apply in the present work the new full-potential augmented spherical wave method to study the electronic properties of the title compounds. We concentrate especially on the strong anisotropies and on the influence of the different species and orbitals on the electronic properties.

2. Theoretical Method

The calculations are based on density-functional theory and the generalized gradient approximation (GGA)[29] with the local-density approximation parametrized according to Perdew and Wang.[30] They were performed using the scalar-relativistic implementation of the augmented spherical wave (ASW) method (see refs 31–33 and references therein). In the ASW method, the wave function is expanded in atom-centered augmented spherical waves, which are Hankel functions and numerical solutions of Schrödinger's equation, respectively, outside and inside the so-called augmentation spheres. In order to optimize the basis set, additional augmented spherical waves were placed at carefully selected interstitial sites. The choice of these sites as well as the augmentation radii were automatically determined using the sphere-geometry optimization algorithm.[34] Self-consistency was achieved by a highly efficient algorithm for convergence acceleration.[35] The Brillouin zone integrations were performed using the linear tetrahedron method with up to 1469 k-points within the irreducible wedge.[36,33]

In the present work, we used a new full-potential version of the ASW method, which was implemented only very recently.[37] In this version, the electron density and related quantities are given by a spherical-harmonics expansion inside the muffin-tin spheres. In the remaining interstitial region, a representation in terms of atom-centered Hankel functions is used.[38] However, in contrast to previous related implementations, we here get away without needing a so-called multiple-κ basis set, which allows for a very high computational speed of the resulting scheme.

(15) Hasegawa, M.; Tanaka, M.; Yagi, T.; Takei, H.; Inoue, A. *Solid State Commun.* **2003**, *128*, 303.
(16) Hasegawa, M.; Inagawa, I.; Tanaka, M.; Shirotani, I.; Takei, H. *Solid State Commun.* **2002**, *121*, 203.
(17) Higuchi, T.; Tsukamoto, T.; Tanaka, M.; Ishii, H.; Kanai, K.; Tezuka, Y.; Shin, S.; Takei, H. *J. Electr. Spectr. Rel. Phen.* **1998**, *92*, 71.
(18) Higuchi, T.; Hasegawa, M.; Tanaka, M.; Takei, H.; Shin, S.; Tsukamoto, T. *Jpn. J. Appl. Phys.* **2004**, *43*, 699.
(19) Mattheiss, L. F. *Phys. Rev. B* **1993**, *48*, 18300.
(20) Galakhov, V. R.; Poteryaev, A. I.; Kurmaev, E. Z.; Anisimov, V. I.; Bartkowski, S.; Neumann, M.; Lu, Z. W.; Klein, B. M.; Zhao, T.-R. *Phys. Rev. B* **1997**, *56*, 4584.
(21) Seshadri, R.; Felser, C.; Thieme, K.; Tremel, W. *Chem. Mater.* **1998**, *10*, 2189.
(22) Ingram, B. J.; Mason, T. O.; Asahi, R.; Park, K. T.; Freeman, A. J. *Phys. Rev. B* **2001**, *64*, 155114.
(23) Nie, X.; Wei, S.-H.; Zhang, S. B. *Phys. Rev. Lett.* **2002**, *88*, 066405.
(24) Kandpal, H. C.; Seshadri, R. *Solid State Sci.* **2002**, *4*, 1045.
(25) Okabe, H.; Matoba, M.; Kyomen, T.; Itoh, M. *J. Appl. Phys.* **2003**, *93*, 7258.
(26) Ong, K. P.; Bai, K.; Blaha, P.; Wu, P. *Chem. Mater.* **2007**, *19*, 634.
(27) Mazin, I. I. *Phys. Rev. B* **2007**, *75*, 094407.
(28) Singh, D. J. *Phys. Rev. B* **2007**, *76*, 085110.
(29) Perdew, J. P.; Burke, K.; Ernzerhof, M. *Phys. Rev. Lett.* **1996**, *77*, 3865.
(30) Perdew, J. P.; Wang, Y. *Phys. Rev. B* **1992**, *45*, 13244.
(31) Williams, A. R.; Kübler, J.; Gelatt, C. D., Jr. *Phys. Rev. B* **1979**, *19*, 6094.
(32) Eyert, V. *Int. J. Quantum Chem.* **2000**, *77*, 1007.
(33) Eyert, V. *The Augmented Spherical Wave Method−A Comprehensive Treatment*; Lecture Notes in Physics; Springer: Berlin, 2007; Vol. 719.
(34) Eyert, V.; Höck, K.-H. *Phys. Rev. B* **1998**, *57*, 12727.
(35) Eyert, V. *J. Comp. Phys.* **1996**, *124*, 271.
(36) Blöchl, P. E.; Jepsen, O.; Andersen, O. K. *Phys. Rev. B* **1994**, *49*, 16223.
(37) Eyert, V. *J. Comput. Chem.* **2008**, in press.

Table 1. Experimental and Calculated Lattice Parameters (in Å) and Atomic Positions

compd		*a*	*c*	*zO*
$PdCoO_2$	expt	2.8300	17.743	0.1112
	calcd	2.8767	17.7019	0.1100
$PtCoO_2$	expt	2.8300	17.837	0.1140
	calcd	2.8989	17.458	0.1128

3. Results and Discussion

Whereas the previous calculations were based on the crystal structure data by Prewitt et al.,[11] we here calculated these parameters from a minimization of the total energy. To this end, in a first step for each compound, the lattice was relaxed and after that the oxygen parameter was optimized. The results for both compounds are summarized in Table 1. Note that the deviation of the calculated structural parameters from the measured ones is 2.4% at most, which is very well within the known limits of the GGA and an excellent proof of the validity of the new full-potential ASW method.

To discuss the electronic properties, we first concentrate on $PdCoO_2$ and only after that discuss the changes coming with the substitution of Pt for Pd. The electronic bands along selected high-symmetry lines of the first Brillouin zone of the hexagonal lattice, Figure 2, are displayed in Figure 3. The corresponding partial densities of states (DOS) are shown in Figure 4. The rather complicated structure of both the electronic bands and the DOS results from the energetical overlap of the relevant orbitals in the energy interval shown. While the lower part of the spectrum is dominated by O 2p states, the transition-metal d states lead to rather sharp peaks in the interval from −3.5 eV to +2 eV. In particular, we recognize the t_{2g} and e_g manifolds of the Co 3*d* states as resulting from the octahedral coordination. In representing these partial DOS we have used a local rotated coordinate system with the Cartesian axes pointing toward the oxygen atoms. σ-type overlap of the O 2p states with the Co 3d e_g orbitals leads to the rather sharp contribution of the latter near −5.8 eV. In contrast, due to the much weaker π-type overlap of the O 2p states with the Co t_{2g} orbitals, these states give rise to sharp peaks in the interval from −2 eV to E_F. Since the Fermi energy falls right between the t_{2g} and e_g manifolds, Co turns out to be in a d^6 low-spin state. Our results thus provide further support to the picture that Co is trivalent, whereas Pd is in a monovalent d^9 configuration.[11–13] Furthermore, the Co and O states give only a tiny contribution to the electrical conductivity, which is maintained almost exclusively by the Pd 4d states. The latter are further analyzed in Figure 5, which displays the five Pd 4d partial DOS. Because Pd is linearly coordinated by two oxygen atoms parallel to the *c* axis and has six Pd neighbors in the *a*−*b* plane we used the global coordinate system to represent these partial DOS. With this choice, contributions from the

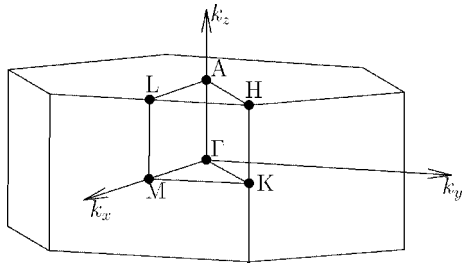

Figure 2. First Brillouin zone of the hexagonal lattice.

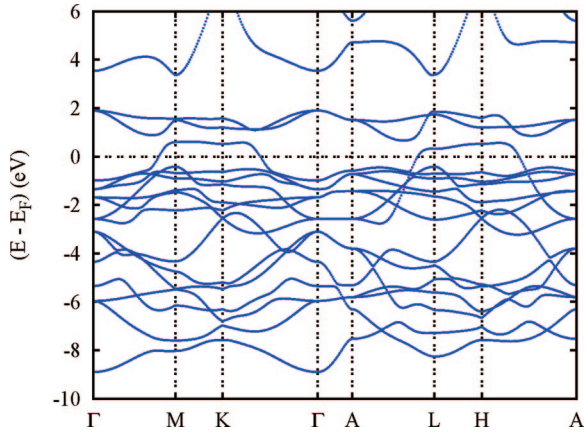

Figure 3. Electronic bands of $PdCoO_2$.

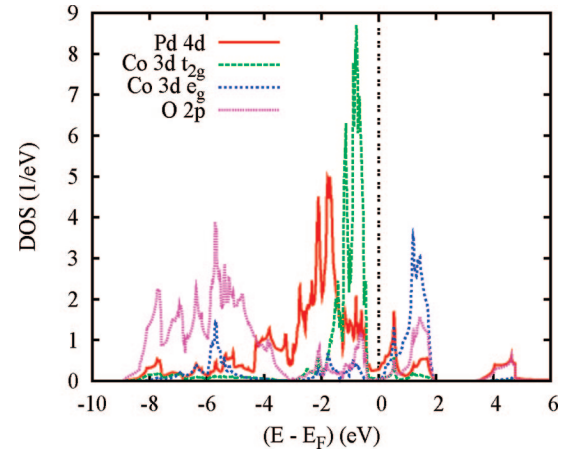

Figure 4. Partial densities of states (DOS) of $PdCoO_2$. Selection of Co 3d orbitals is relative to the local rotated reference frame, see text.

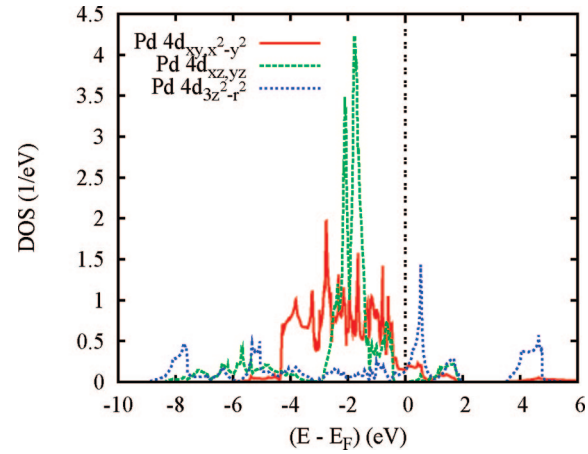

Figure 5. Partial Pd 4d DOS of $PdCoO_2$.

(38) Methfessel, M. S. *Phys. Rev. B* **1988**, *38*, 1537.
(39) Kokalj, A. *Comput. Mater. Sci.* **2003**, *28*, 155.

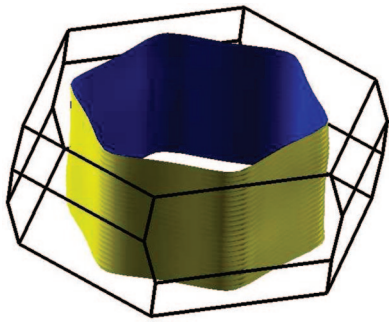

Figure 6. Fermi surface of $PdCoO_2$.

d_{xy} and $d_{x^2-y^2}$ as well as from the d_{xz} and d_{yz} states are identical. The Pd 4d partial DOS are strongly influenced by the aforementioned coordination. In particular, the six peaks of the $d_{3z^2-r^2}$ states near −8.0, −6.2, −5.2, +0.6, 1.5, and +4.2 eV are complemented by contributions of the O 2p partial DOS of similar shape reflecting the strong σ-type d−p overlap along the *c* axis. In contrast, the short in-plane Pd-Pd distances of about 2.83Å (experimental value), which are only by 3% longer than those in metallic Pd, lead to the broad Pd d_{xy,x^2-y^2} bands visible in the interval from −4.5 to 2 eV in Figure 5. In addition, these bands give rise to the largest contribution at E_F, whereas the $d_{xz,yz}$ states do not contribute at all. In contrast, the contribution from the $d_{3z^2-r^2}$ orbitals is rather similar to that of the d_{xy,x^2-y^2} orbitals. However, according to a *k*-resolved analysis, their weights vary on the Fermi surface. At about +0.6 eV, the contribution of the d_{xy,x^2-y^2} orbitals is strongly suppressed, and the small dispersion along the line M−K causes the sharp $d_{3z^2-r^2}$ peak seen in Figure 5.

The strong quasi two-dimensionality of the electronic states is reflected by the Fermi surface depicted in Figure 6. Apart from the very small bending parallel to the *c* direction, it gives rise to completely in-plane Fermi velocities and explains the strong anisotropy in electric conductivity. However, note that according to the electronic bands shown in Figure 3, the dispersion parallel to the direction Γ−A in general is not negligible. In passing, we mention the negligible dispersion along M−K, which is typical of tight-binding bands in a triangular lattice. These bands give rise to the sharp peak at about +0.6 eV in Figure 5 and can thus be attributed to the Pd $d_{3z^2-r^2}$ states.

Overall, our results are in good agreement with the previous calculations by Seshadri et al. and by Okabe et al.[21,25] In particular, Seshadri et al. obtained a distribution of states at E_F, which is similar to ours. Furthermore, our results are in agreement with the photoemission data by Tanaka et al. and Higuchi et al.,[12,17] who attribute the metallic conductivity almost exclusively to the Pd 4d states. It has been argued by several authors, that the dominant contribution is due to the Pd $d_{3z^2-r^2}$ orbitals, which hybridize with the Pd 5s states. Although we find indeed a 5s contribution of the order of 0.02 states/eV, hence, on the order of 10% of the $d_{3z^2-r^2}$ partial DOS at E_F, we still point to the in-plane d_{xy} and $d_{x^2-y^2}$ states, which play an even greater role at E_F than the $d_{3z^2-r^2}$ states. As a consequence, our results demonstrate that the metallic conductivity is maintained by the in-plane d_{xy} and $d_{x^2-y^2}$ orbitals and the in-plane part of the $d_{3z^2-r^2}$ orbitals to a similar degree with a somewhat greater influence of the former. This finding is confirmed by the calculations for $PtCoO_2$, where the DOS at E_F is again almost exclusively due to the in-plane states.

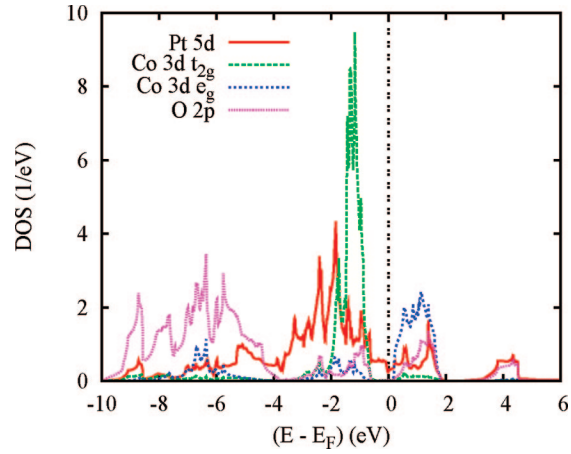

Figure 7. Partial densities of states (DOS) of $PtCoO_2$. Selection of Co 3d orbitals is relative to the local rotated reference frame, see text.

In general, the partial DOS obtained for $PtCoO_2$, which are displayed in Figure 7, resemble those of the palladium system. However, the larger extent of the Pt 5d orbitals as compared to the Pd 4d states leads to an increased width mainly of the in-plane d bands as well as an increased overlap of these states with the O 2*p* states. As a consequence, the anisotropy of the electrical conductivity will be somewhat reduced in $PtCoO_2$ as is indeed observed.[11]

In passing, we mention additional GGA+U calculations for $PdCoO_2$, which, however, confirmed the GGA results without any noticeable changes.

4. Summary

In summary, we have shown that the strongly anisotropic metallic conductivity of $PdCoO_2$ and $PtCoO_2$ is almost exclusively due to the Pd (Pt) layers. In contrast, the octahedrally coordinated CoO_2 sandwiches are insulating. As Co was found in a low-spin d^6 configuration, these CoO_2 complexes strongly suppress the electronic coupling between the Pd (Pt) metallic layers, and the Co^{3+} layers merely act as charge reservoirs. In addition, they pronounce the quasi two-dimensionality of the system. It may be speculated how the introduction of impurities into the cobalt layers, i.e. replacing, e.g., Fe or Ni for Co, alters the electronic properties locally and might thus be used to design nanostructured materials. Work along this line is in progress. In this context, one might ask to what extent the structural changes induced by the introduction of impurities with different covalent radii as compared to Co might be damped by the intermediate oxygen layers. This would provide a situation, where chemical substitution only acts on the electronic degrees of freedom.

Acknowledgment. We gratefully acknowledge many fruitful discussions with T. Kopp, C. Martin, and W. C. Sheets. This work was supported by the Deutsche Forschungsgemeinschaft through SFB 484. Figures 1 and 6 were generated using the XCrysDen software (ref 39).

CM703404E